Published OnlineFirst April 4, 2018; DOI: 10.1158/1078-0432.CCR-17-3657

Precision Medicine and Imaging

Clinical Cancer Research

Inositol Trisphosphate Receptor Type 3-mediated Enhancement of EGFR and MET Cotargeting Efficacy in Non–Small Cell Lung Cancer Detected by ^{18}F-fluorothymidine

Francesca Iommelli[1,2], Viviana De Rosa[1,2], Cristina Terlizzi[3], Marcello Monti[3], Mariarosaria Panico[1], Rosa Fonti[1], and Silvana Del Vecchio[1,3]

Abstract

Purpose: Our aim was to test whether imaging with ^{18}F-fluorothymidine (^{18}F-FLT) PET/CT was able to detect the combined effects of EGFR and MET inhibitors in oncogene-driven non–small cell lung cancer (NSCLC) and to elucidate the mechanisms underlying the enhanced efficacy of drug combination.

Experimental Design: NSCLC cells bearing *MET* amplification (H1993 and H820) were treated with EGFR and MET inhibitors either alone or in combination and then tested for cell viability and inhibition of signaling. Nude mice bearing H1993 tumors underwent ^{18}F-FLT PET/CT scan before and after treatment with erlotinib and crizotinib alone or in combination (1:1 ratio) and posttreatment changes of ^{18}F-FLT uptake in tumors were determined. The role of inositol trisphosphate receptor type 3 (IP3R3) in mediating the combined action of EGFR and MET inhibitors was tested by transfecting NSCLC cells with IP3R3-targeted siRNA.

Results: Imaging studies showed a significant reduction of ^{18}F-FLT uptake in response to combined treatment with EGFR and MET inhibitors that was higher than that obtained with single agents (ANOVA, F-ratio = 6.215, $P = 0.001$). Imaging findings were confirmed by analysis of surgically excised tumors. Levels of IP3R3 were significantly reduced in both cells and tumors after treatment with crizotinib, whereas EGFR inhibitors caused a reduction of IP3R3 interaction with K-Ras mainly through dephosphorylation of serine residues of K-Ras.

Conclusions: Our findings indicate that ^{18}F-FLT PET/CT is able to detect the enhanced efficacy of EGFR and MET inhibitors in oncogene-driven NSCLC and that such enhancement is mediated by IP3R3 through its interaction with K-Ras. *Clin Cancer Res; 24(13); 3126–36. ©2018 AACR.*

Introduction

Genetic alterations causing neoplastic transformation usually drive a reprogramming of the whole signaling network in order to support cancer cell proliferation, survival, metabolism, migration, and invasion. A number of genetic aberrations have been indeed identified as triggers of neoplastic transformation and the term "oncogene addiction" indicates the dependence of certain tumors from one or few genes for the maintenance of their malignant phenotype (1–3). Once an oncogene driver has been identified, it becomes an optimal target for therapy since its inhibition causes tumor cell death. However, prolonged and selective pharmacological inhibition of an oncogene driver may promote the adoption of compensatory signaling pathways or the occurrence of molecular events altering target structure with a consequent rearrangement of intracellular signaling network which ultimately result in drug resistance (4, 5). Therefore, simultaneous inhibition of multiple signaling pathways emerged as a potentially effective strategy to obtain a durable targeted therapeutic control of cancer in individual patients (6). The rational combination of two or more targeted agents is based on genomic profiling of single tumors that may identify the primary driver oncogene and key targets in possible compensatory mechanisms (5, 7).

The *EGFR* has been recognized as a driver of non–small cell lung cancer (NSCLC) and served as a paradigm for tumor targets that can be successfully inhibited by specific tyrosine kinase inhibitors (TKI) or antagonists with a consequent clinical benefit for the patient (8). The presence of activating mutations in the kinase domain of EGFR is indeed the major determinant of effective tumor response to EGFR TKIs and therefore patients with advanced NSCLC bearing such mutations are candidate to first line therapy with gefitinib or erlotinib (9, 10). Although a high response rate to EGFR TKIs was reported in patients with advanced EGFR-mutant NSCLC with an improvement of progression-free survival (11), the majority of these patients will subsequently become refractory to treatment with EGFR TKIs due to the occurrence of secondary mutation of EGFR such as T790M or redundant lateral signaling through amplification of MET receptor (4, 12–14). These mechanisms are not mutually exclusive and may coexist in the same tumor (15–18).

[1]Institute of Biostructures and Bioimaging, National Research Council, Naples, Italy. [2]CEINGE-Advanced Biotechnologies, Naples Italy. [3]Department of Advanced Biomedical Sciences, University "Federico II", Naples, Italy.

Note: Supplementary data for this article are available at Clinical Cancer Research Online (http://clincancerres.aacrjournals.org/).

Corresponding Author: Silvana Del Vecchio, University of Naples Federico II, Via S. Pansini, 5-Edificio 10, Napoli 80131, Italy. Phone: 39-081-7463307; Fax: 39-081-5457081; E-mail: delvecc@unina.it

doi: 10.1158/1078-0432.CCR-17-3657

Published OnlineFirst April 4, 2018; DOI: 10.1158/1078-0432.CCR-17-3657

Translational Relevance

Cotargeting of EGFR and MET receptors in patients with oncogene-driven non–small cell lung cancer (NSCLC) is a strategy currently adopted in clinical trials to potentially improve therapeutic benefit. Here we showed that combined therapy with EGFR and MET inhibitors in erlotinib resistant NSCLC caused an enhancement of drug effects and this enhancement could be detected and quantitatively analyzed using ^{18}F-fluorothymidine and positron emission tomography. Furthermore, we provided consistent evidences that the enhanced efficacy of EGFR and MET inhibitors is mediated by inositol trisphosphate receptor type 3 (IP3R3) and its interaction with K-Ras. The major translational relevance of this study is to provide a noninvasive imaging tool to assess the enhanced efficacy of EGFR and MET cotargeting and to highlight the role of IP3R3 in enhancing the effects of drug combination so that it can be taken into account for the rational combination of targeted agents.

MET is a receptor tyrosine kinase that, upon binding to its ligand hepatocyte growth factor (HGF), activates a signaling cascade mainly mediated by the RAS-MAPK and PI3K-AKT pathways, which ultimately results in cell-cycle progression, survival, and enhanced cell motility (19–21). Aberrant expression or constitutive activation of MET was found in a considerable percentage of NSCLC and was reported to be associated with a poor outcome (22, 23). A common cause of receptor overexpression and constitutive activation is *MET* gene amplification that can be intrinsically present in primary untreated tumors and/or emerge as a compensatory mechanism in NSCLC exposed to the selective drug pressure of EGFR TKIs (13, 19, 24).

Simultaneous targeting of EGFR and MET receptors with combination of selective inhibitors in patients with NSCLC is a strategy currently tested in clinical trials to improve therapeutic benefit in term of progression free and overall survival, to prevent the emergence of preexisting resistant clones in response to EGFR inhibitors and to overcome MET-mediated resistance with or without T790M secondary mutation in EGFR-driven NSCLC (25–27). Our previous studies showed that imaging with ^{18}F-fluorothymidine (^{18}F-FLT) and PET/CT may identify, early in the course of treatment with single agent, tumors that are sensitive or resistant to EGFR TKIs (28–30). Furthermore, in models of *MET* amplification and T790M-mediated resistance, ^{18}F-FLT PET/CT was able to monitor the reversal of resistance in response to treatment with crizotinib (28) or WZ4002 (29), respectively. The aim of this study was to test whether ^{18}F-FLT PET/CT was able to detect the combined effects of EGFR and MET inhibitors in the treatment of refractory NSCLCs and to elucidate the mechanisms underlying the enhanced efficacy of such drug combination.

Materials and Methods

Cell lines and treatment

NSCLC cells bearing *MET* amplification with mutant or wild-type *EGFR* were obtained from and authenticated by American Type Culture Collection. In particular, H1993 cells are reported to have 15 copies of *MET* gene and wild-type *EGFR* whereas H820 cells show six copies of *MET* gene and double-mutant *EGFR*, that is, deletion in exon 19 (delE746_E749) and T790M secondary mutation (18, 31). Both cell lines were resistant to erlotinib. All cells were grown in RPMI medium containing 10% FBS, 100 IU/mL penicillin, and 50 μg/mL streptomycin in a humidified incubator in 5% CO_2 at 37°C.

H1993 cells were treated with erlotinib and crizotinib (Selleck Chemicals), a potent MET inhibitor currently used in clinical trials, at the indicated doses alone or in combination. H820 cells, bearing concurrent mechanisms of resistance to EGFR TKIs, were treated with crizotinib and WZ4002 (Selleck Chemicals), an irreversible inhibitor with a high affinity for T790M-mutant EGFR, alone or in combination. In all *in vitro* experiments, the combination of the two agents was performed using a constant dose ratio of 1:1 so that the combined dose was equivalent to that of the single agent.

Drug-induced toxicity was assessed by using the MTS assay (Promega) as previously described (28). Briefly, NSCLC cells were treated for 72 hours at 37°C with increasing concentration (range 0.01–10 μmol/L) of each agent alone or in combination. After the addition of MTS, the percentage of viable cells was determined considering the untreated control cells as 100%. At least three independent experiments were performed in triplicates and data were pooled.

Western blot analysis and immunoprecipitation

Whole cell lysates were prepared as previously described (28, 32). Briefly, cells were treated with EGFR and MET inhibitors alone (0.5 and 1 μmol/L) or in combination (1:1 ratio) for 6 hours or 24 to 72 hours at 37°C. Untreated and treated cells were lysed on ice in RIPA lysis buffer with protease and phosphatase inhibitors (Sigma-Aldrich). The suspension was then homogenized by passages through a 26-gauge needle and centrifuged at 13,000 × *g* for 30 minutes at 4°C. Western blot analysis of proteins from whole cell lysates was carried out using a standard procedure. Polyvinylidene difluoride (PVDF) membranes were probed by using monoclonal antibodies recognizing phospho-EGFR, MET (25H2), p42/44 MAP kinase, phospho-p42/44 MAP kinase (Thr202/Tyr204), STAT3 (Cell Signaling; 0.1 μg/mL), IP3R3, PARP (BD Biosciences; 0.25 μg/mL), K-Ras, Bcl-xL (Santa Cruz Biotechnology; 0.2 μg/mL), actin, α-tubulin (Sigma; 1 μg/mL), and rabbit polyclonal antibodies specific for EGFR, phospho-AKT (Ser473 Santa Cruz Biotechnology; 1:1,000), AKT, cyclin D1, phospho-MET (Tyr 1234/1235), phospho-STAT3^{Tyr705}, c-Myc, cleaved PARP (Asp214; Cell Signaling; 1:1,000), phospho-serine (Enzo Life Sciences, 2 μg/mL), and BIM (Calbiochem, 1:1,000).

Immunoprecipitation was performed as previously described (33). Briefly, precleared proteins from cell lysates (1 mg) were incubated overnight at 4°C with 4 μg/mL of anti-IP3R3 monoclonal antibodies (BD Biosciences). The immunoprecipitated proteins recovered by absorption to EZview Red Protein A Affinity Gel (Sigma-Aldrich) were separated by SDS-PAGE, transferred to PVDF membranes, and probed for the indicated proteins. Three independent experiments were performed.

Cell-cycle analysis

Flow cytometry was used for cell-cycle analysis (29). Briefly, cells were treated with crizotinib, erlotinib or WZ4002 at 0.5 and 1 μmol/L either alone or in combination for 24 hours at 37°C. After treatment, cells were collected and washed with

Published OnlineFirst April 4, 2018; DOI: 10.1158/1078-0432.CCR-17-3657

cold PBS and fixed in ice-cold ethanol 95% (v/v). After two rinses in PBS, 1×10^6 cells were stained with propidium iodide (5 μg/mL) in the presence of RNase (25 μg/mL; Sigma-Aldrich) overnight at 4°C in the dark and analyzed by fluorescence-activated cell sorting (BD FACSAria II). At least three independent experiments were performed in triplicate, data were analyzed using a Mod-Fit III (Verity) cell-cycle analysis program.

Animal tumor models and treatment

Female BALB/c (nu/nu) mice, 6 weeks old, weighing 15 to 20 g were purchased from Charles River Laboratories (Milan, Italy). All animal experimental procedures were approved by the Italian Ministry of Health-Animal Welfare Direction (Protocol No. DGSAF21940-A-16/11/2013 and authorization No. 324/2017-PR 18/04/2017). H1993 cells ($5–10 \times 10^6$) were resuspended in 200 μL RPMI medium and injected subcutaneously into the flank of nude mice. Cells were then allowed to grow and when tumors reached a mean volume of approximately 100 mm^3 [volume = 0.5 × greatest diameter × (shortest diameter)^2] animals were randomized into treatment groups (of at least four animals for each treatment and dose): group 1, vehicle; group 2, 50 mg/kg crizotinib; group 3, 50 mg/kg erlotinib; group 4, 25 mg/kg crizotinib plus 25 mg/kg erlotinib; group 5, 100 mg/kg crizotinib; group 6, 100 mg/kg erlotinib; group 7, 50 mg/kg crizotinib plus 50 mg/kg erlotinib. Animals were treated daily for 3 days by oral gavage.

Imaging studies with ^{18}F-FLT and small-animal PET/CT

The whole synthesis of ^{18}F-FLT was performed as previously described (28, 34) and the resulting labeled products had >99% radiochemical purity as assessed by high-performance liquid chromatography.

Each animal underwent a baseline and a posttreatment scan. Animals were intravenously injected with 7.4 MBq of ^{18}F-FLT and after 50 minutes were anaesthetized and subjected to imaging studies using a small-animal PET/CT scanner (eXplore Vista Pre-Clinical PET Scanner GE Healthcare). CT scan was performed using the following parameters: 35 kVp and 200 μA. One bed position including the tumor was scanned for 10 minutes with an axial field of view of 68 mm. PET images were then acquired at 1-hour post-injection for an acquisition time of 20 minutes. Body temperature of animals was held constant during tracer biodistribution and imaging using a heating pad or heat lamp. Reconstructed PET images were corrected for decay and converted to SUV. No statistically significant change of animal weight was observed after 3-day treatment. Three-dimensional regions of interest were drawn around the tumor on transaxial PET images and a volume of interest was determined using an automated isocontoring program (28, 35). The maximum voxel value of SUV within the tumor volume of interest was then registered for each study. Finally, the percentage change of ^{18}F-FLT uptake in the post-treatment study as compared to baseline scan was determined in each animal. All quantitative data from animal imaging studies were expressed as mean ± SE.

Signaling mediators, rate of proliferation and markers of apoptosis in tumor xenografts

At the end of imaging studies, tumors obtained from animals were homogenized on ice in RIPA lysis buffer containing protease and phosphatase inhibitors (Sigma-Aldrich) using a dounce homogenizer (28, 36). The suspension was clarified by centrifugation at 13,000 × *g* for 30 minutes at 4°C and subjected to Western blotting for the analysis of p-AKT/AKT, p-ERK1/2/ERK1/2, p-STAT3^{Tyr705}/STAT3, c-Myc, cyclin D1, IP3R3, BIM, Bcl-xL, PARP, and cleaved PARP levels.

To determine the rate of proliferation, 5 μm adjacent frozen sections were immunostained with the rabbit polyclonal antibody recognizing Ki67 antigen (Abcam, dilution 1:100) as previously described (29). Tumor sections were examined by light microscopy at ×400 magnification and the results were expressed as the mean percentage of positively stained tumor cells in a section. Data from treated tumors (at least three for each group of treatment) were averaged and compared to data from vehicle treated tumors ($n = 3$) by unpaired Student *t* test.

RNA interference

IP3R3-targeted siRNA pool (ON-TARGETplus SMARTpool siRNA ITPR3) and control nontargeting siRNA pool (scrambled) were purchased from Dharmacon Inc., and used according to the manufacturer's instructions. Briefly, H1993 cells were plated at 40% confluence in medium supplemented with 10% FBS and allowed to attach for 24 hours. Cells were then transfected with 100 nmol/L siRNAs using Dharmafect reagent (Dharmacon), as previously described (32). After 48 hours, cells were treated with 1 μmol/L erlotinib, 1 μmol/L crizotinib, or vehicle for 24 hours and then lysed for Western blot analysis. Three independent experiments were performed.

Ras activation assay

Levels of GTP-bound Ras were tested using a commercially available Ras Activation Kit (Millipore) according to the manufacturer's protocol. Briefly, H1993 cells were starved overnight and then treated with crizotinib (1 μmol/L) and erlotinib (1 μmol/L) alone or in combination for 24 hours at 37°C. Pull-down of active Ras from cell lysates (1,000 μg) was performed using Ras-binding domain of Raf-1 conjugated to glutathione agarose beads. Precipitated samples were subjected to SDS-PAGE and western blotting with anti-Ras antibody (Millipore; 1:1,000). Three independent experiments were performed.

Statistical analysis and combination index

Statistical analysis was performed using the software MedCalc for Windows, version 10.3.2.0, (MedCalc Software, Mariakerke, Be). Paired Student *t* test was used to compare means of ^{18}F-FLT uptake in the same tumors before and after treatment. ANOVA followed by pairwise comparisons was used to assess differences among multiple treatment groups. A value of $P < 0.05$ was considered statistically significant.

The effects of the combined treatment were analyzed using the CompuSyn software program based on the Chou and Talalay method (37, 38). Dose–effect curves were generated for each data set and the combination index (CI) was then calculated. A value of CI < 1, CI = 1, or CI > 1 indicates synergism, additivity, or antagonism, respectively. In general, the smaller is the CI value, the greater is the strength of synergy.

Results

Toxicity of combined treatment with EGFR and MET inhibitors

To select a cell line suitable for *in vivo* imaging studies, cell toxicity of increasing concentrations of EGFR TKIs and

Published OnlineFirst April 4, 2018; DOI: 10.1158/1078-0432.CCR-17-3657

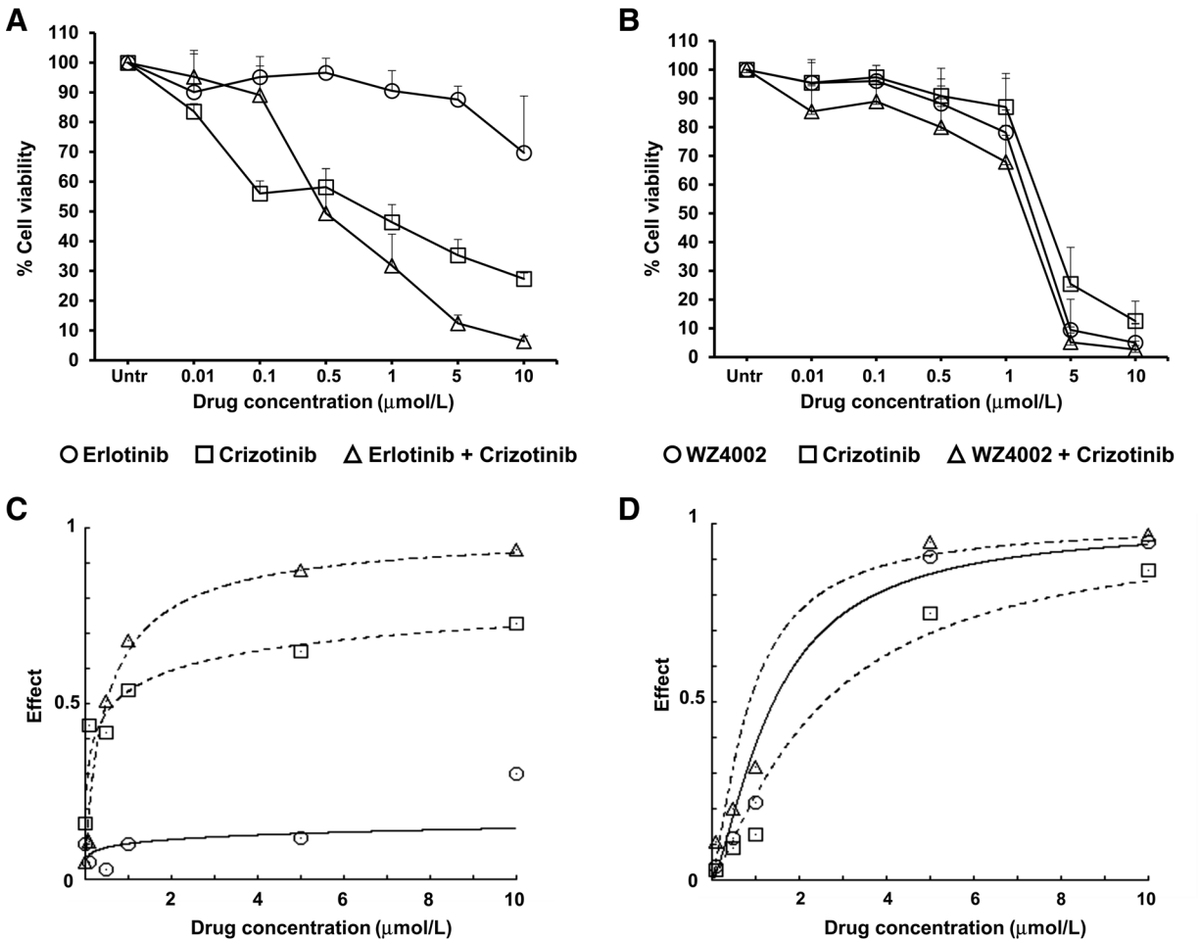

Figure 1.

Toxicity of combined treatment with EGFR and MET inhibitors. **A** and **B,** cell toxicity was determined by MTS assay in H1993 (**A**) and H820 (**B**) cells treated with increasing doses of EGFR and MET inhibitors used alone or in combination at 1:1 ratio for 72 hours. **C** and **D,** dose-effect curves were generated for H1993 (**C**) and H820 (**D**) cells and values of CI <1 were obtained indicating a synergistic effect at different concentrations. At least three independent experiments were performed and data are expressed as mean ± SE.

crizotinib alone or in combination was preliminary tested by MTS assay in H1993 and H820 cells. The percentage of viable cells at different dose levels were used to calculate the CI. Fig. 1A shows the results obtained in H1993 cells exposed to erlotinib, crizotinib or combination of both agents whereas in Fig. 1B H820 cells were treated with WZ4002 and crizotinib alone or in combination, since the presence of concurrent mechanisms of resistance in these cells prevented the use of erlotinib and crizotinib (Supplementary Fig. S1). As expected, H1993 cells were resistant to erlotinib at the concentration used whereas treatment with crizotinib showed a reduction of cell viability indicating drug sensitivity (Fig. 1A). The combination of crizotinib and erlotinib (1:1 ratio) caused an enhanced cell toxicity as compared to treatment with single agent at cumulative doses higher than 0.5 μmol/L. CI values derived from dose/effects curves (Fig. 1C) were <1 in the interval of cumulative doses between 0.5 and 10 μmol/L indicating synergism. Although to a lesser extent, even H820 cells showed a higher level of growth inhibition after combined treatment with WZ4002 and crizotinib (1:1 ratio) as compared to exposure to single agent at all drug concentrations. CI values derived from dose/effects curves (Fig. 1D) were <1 indicating synergism.

Effects of combined treatment on EGFR and MET signaling

Whole cell lysates from H1993 (Fig. 2A) and H820 (Fig. 2B) cells were tested for levels of total and phosphorylated EGFR, MET, AKT, and ERK 1/2 as well as cyclin D1 by Western blotting upon 6 hours exposure to vehicle, single agent, or drug combination. In H1993 cells, treatment with crizotinib alone reduced the levels of all signaling mediators and cyclin D1 although they remained detectable at the indicated doses (Fig. 2A). Despite the reduced levels of p-EGFR, erlotinib alone did not cause any detectable changes in the levels of EGFR signaling mediators. The combined treatment of crizotinib and erlotinib (1:1 ratio) caused a strong reduction of all phosphorylated forms of signaling mediators and cyclin D1 so that their levels were almost undetectable at the indicated cumulative doses (Fig. 2A). In agreement with these findings, cell-cycle analysis showed the highest G_1–S ratio in response to combined treatment indicating the maximal

Published OnlineFirst April 4, 2018; DOI: 10.1158/1078-0432.CCR-17-3657

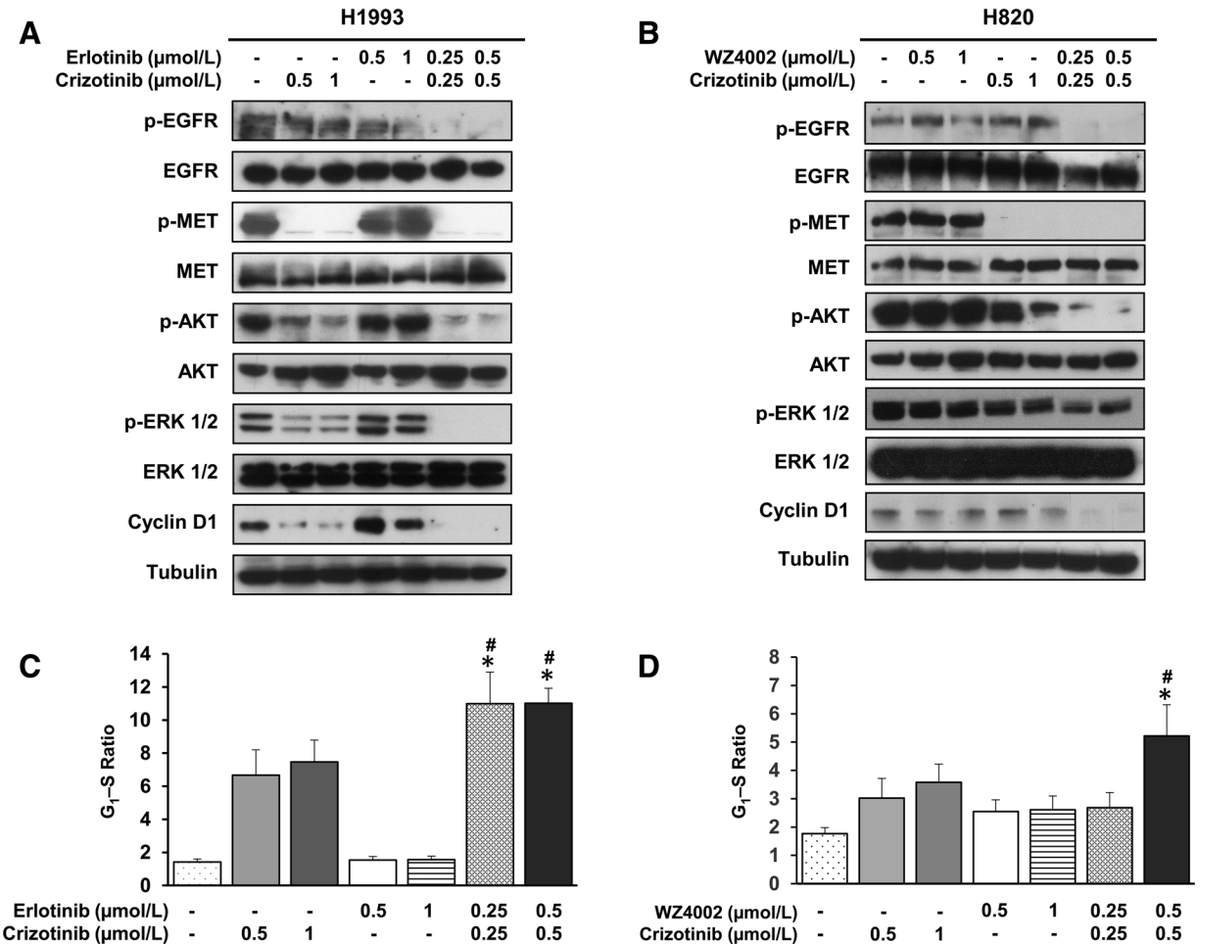

Figure 2.

Signaling cascade and cell-cycle analysis in response to combined treatment. **A** and **B,** Western blot analysis of whole cell lysates was performed in H1993 (**A**) and H820 (**B**) cells. Levels of the indicated proteins were tested after 6 hours treatment with EGFR and MET inhibitors used alone or in combination. Tubulin was used to ensure equal loading. **C** and **D,** cell-cycle analysis was performed in H1993 (**C**) and H820 (**D**) cells after 24 hours treatment with single agents or drug combination. At least three independent experiments were performed and data are expressed as mean ± SE (*, $P < 0.05$ combined treatment vs. 0.5 μmol/L crizotinib; #, $P < 0.05$ combined treatment vs. 1 μmol/L crizotinib).

effect on growth arrest (Fig. 2C). Analysis of variance followed by pairwise comparisons showed a statistically significant difference in G_1–S ratio among multiple treatment groups (F-ratio = 16.99, $P < 0.001$). In particular, G_1–S ratio was significantly higher ($P < 0.05$) in cells treated with drug combination as compared to those exposed to single agent at the same cumulative doses.

Similar results were obtained by western blot analysis (Fig. 2B) and cell-cycle evaluation (Fig. 2D) in H820 cells treated with WZ4002 and crizotinib alone or in combination (1:1 ratio). In particular, the G_1–S ratio after treatment of H820 cells with high dose drug combination was significantly higher ($P < 0.05$) than that found in cells exposed to single agent at the indicated doses.

Imaging of EGFR and MET cotargeting by ^{18}F-FLT PET/CT

Nude mice bearing H1993 tumors were subjected to ^{18}F-FLT PET/CT scan at the baseline and after treatment with erlotinib and crizotinib alone or in combination (1:1 ratio) at the same cumulative doses. As shown in Fig. 3A and B (top), treatment with erlotinib at low (50 mg/kg) and high (100 mg/kg) dose regimen did not cause any change of ^{18}F-FLT uptake in tumors whereas low (50 mg/kg) and high (100 mg/kg) dose treatment with crizotinib showed a strong reduction of tracer uptake in xenografts (Fig. 3A and B, middle). When combined treatment was administered to animals at cumulative doses of 25 mg/kg crizotinib plus 25 mg/kg erlotinib (Fig. 3A, bottom) or 50 mg/kg crizotinib plus 50 mg/kg erlotinib (Fig. 3B, bottom), tumors showed a strong ^{18}F-FLT uptake reduction comparable to that caused by crizotinib alone at the corresponding cumulative dose.

Quantitative analysis was performed on ^{18}F-FLT PET/CT images and mean SUV_{max} values of tumors in pre- and post-treatment scans are reported in Fig. 4A for each group of animals. A statistical significant reduction of ^{18}F-FLT uptake was observed in tumors of all treatment groups except those receiving 50 and 100 mg/Kg erlotinib alone. Fig. 4B shows the percentage variation of ^{18}F-FLT uptake in tumors before

Published OnlineFirst April 4, 2018; DOI: 10.1158/1078-0432.CCR-17-3657

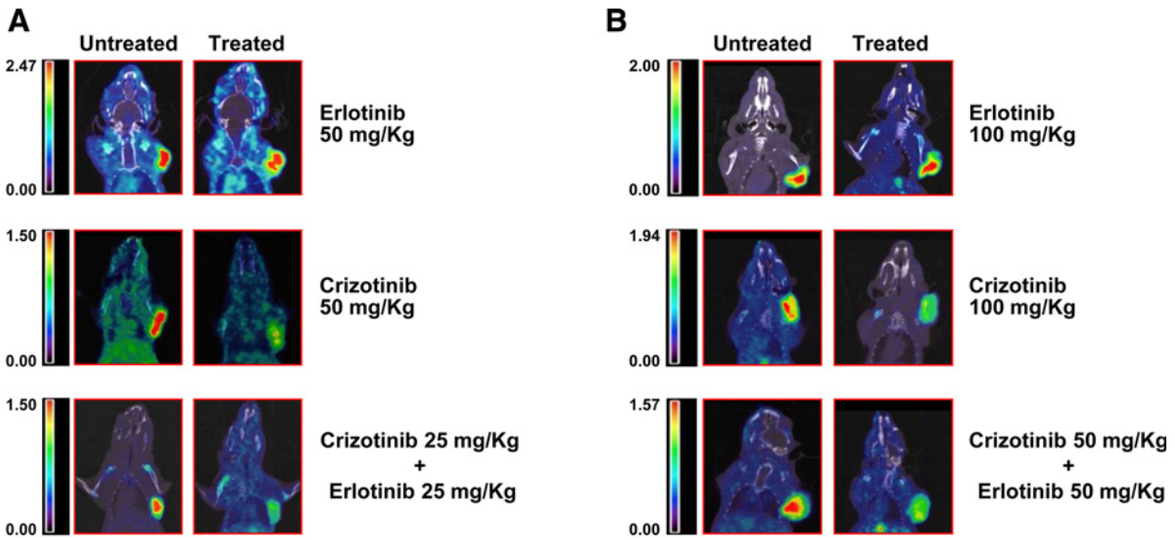

Figure 3.

In vivo evaluation of tumor response to EGFR and MET inhibitors by ^{18}F-FLT PET/CT. **A** and **B,** Nude mice bearing H1993 xenografts were studied with ^{18}F-FLT PET/CT before and after 3 days treatment with erlotinib or crizotinib alone or in combination at cumulative doses of 50 mg/kg (**A**) and 100 mg/kg (**B**). Representative images of the same animal before and after therapy are shown.

and after treatment of each animal with single agents or drug combination at the indicated doses. In particular, tumor-bearing mice treated with 50 mg/kg crizotinib showed a mean reduction of tracer uptake of 27.32% ± 8.56% whereas treatment with 100 mg/kg crizotinib caused a reduction of tracer uptake of 43.80% ± 3.34%. No significant changes of ^{18}F-FLT uptake was found in tumors exposed to low and high dose erlotinib. Combination therapy with 25 mg/kg crizotinib plus 25 mg/kg erlotinib induced a reduction in tracer uptake of 41.40% ± 5.56% whereas combined regimen with 50 mg/kg crizotinib plus 50 mg/kg erlotinib caused a reduction of 44.73% ± 3.68% in tumor uptake of ^{18}F-FLT. Analysis of variance for comparison among multiple treatment groups showed a statistically significant difference in changes of ^{18}F-FLT uptake in response to therapy (F-ratio = 6.215, $P = 0.001$). In particular, the reduction of ^{18}F-FLT uptake after low dose combined treatment (25 mg/kg crizotinib plus 25 mg/kg erlotinib) was significantly higher ($P < 0.05$) than that achieved after therapy with 50 mg/kg crizotinib or erlotinib alone. Furthermore high-dose combination therapy (50 mg/kg crizotinib plus 50 mg/kg erlotinib) caused a reduction of ^{18}F-FLT uptake significantly higher than that induced by 50 mg/kg crizotinib and 100 mg/kg erlotinib alone and not significantly different from that obtained after 100 mg/kg crizotinib alone. The CI values derived from dose/effects curves were 0.274 and 0.483 for low- and high-dose combination regimen, indicating synergism between crizotinib and erlotinib in reducing ^{18}F-FLT uptake.

In agreement with imaging findings, levels of cyclin D1 in excised tumors were maximally reduced by combination therapy with 50 mg/kg crizotinib plus 50 mg/kg erlotinib (Fig. 4C). A further confirmation of imaging findings was provided by Ki67 staining of tumor sections from surgically removed xenografts (Fig. 4D). Analysis of variance showed a statistically significant difference in rate of proliferation among multiple treatment groups (F-ratio=17.36, $P < 0.001$). In particular, the rate of proliferation was significantly lower in tumor treated with low dose combination regimen as compared to that obtained after treatment with 50 mg/kg crizotinib alone ($P < 0.05$). Similarly, the percentage of Ki67 positive cells was significantly lower in tumors treated with high dose combination treatment than in xenografts exposed to 50 mg/kg ($P < 0.05$) or 100 mg/kg ($P < 0.05$) crizotinib alone.

Molecular mechanisms of enhanced efficacy of EGFR and MET cotargeting

To elucidate which signaling pathways and mechanisms are involved in the enhancement of combined effects of EGFR and MET inhibitors, we tested levels of p-AKT, p-ERK1/2, p-STAT3^{Tyr705}, c-Myc, and markers of apoptosis such as BIM, Bcl-xL, and PARP by Western blot analysis of excised tumors after 3 days of treatment. Fig. 5A shows that combined treatment of animals with erlotinib and crizotinib caused a reduction of the phosphorylated forms of signaling mediators and effectors that resulted to be higher than that achieved with crizotinib and erlotinib alone. Fig. 5B shows a slight increase of BIM levels in specimens treated with single agents for 3 days and also a slight increase of cleaved PARP levels in tumors exposed to combined regimen. Because the enhanced efficacy of EGFR and MET inhibitors on proliferation was simultaneously observed in AKT, MAPK, and STAT pathways, we hypothesized that the modulation of an upstream target through an additional parallel pathway could eventually generate a synergy. Binding of both EGFR and MET receptor with their own ligands may induce an increase of inositol trisphosphate and an enhancement of its interaction with inositol trisphosphate receptor (IP3R), a calcium channel expressed on the membrane of endoplasmic reticulum (39). Therefore we tested the levels of IP3R3, the major isoform expressed in malignant tumors (40), in response to erlotinib and crizotinib alone or in combination. Fig. 5C shows a dramatic reduction of IP3R3 levels in tumor samples from animals treated with crizotinib alone or in combination with erlotinib for 3 days

Published OnlineFirst April 4, 2018; DOI: 10.1158/1078-0432.CCR-17-3657

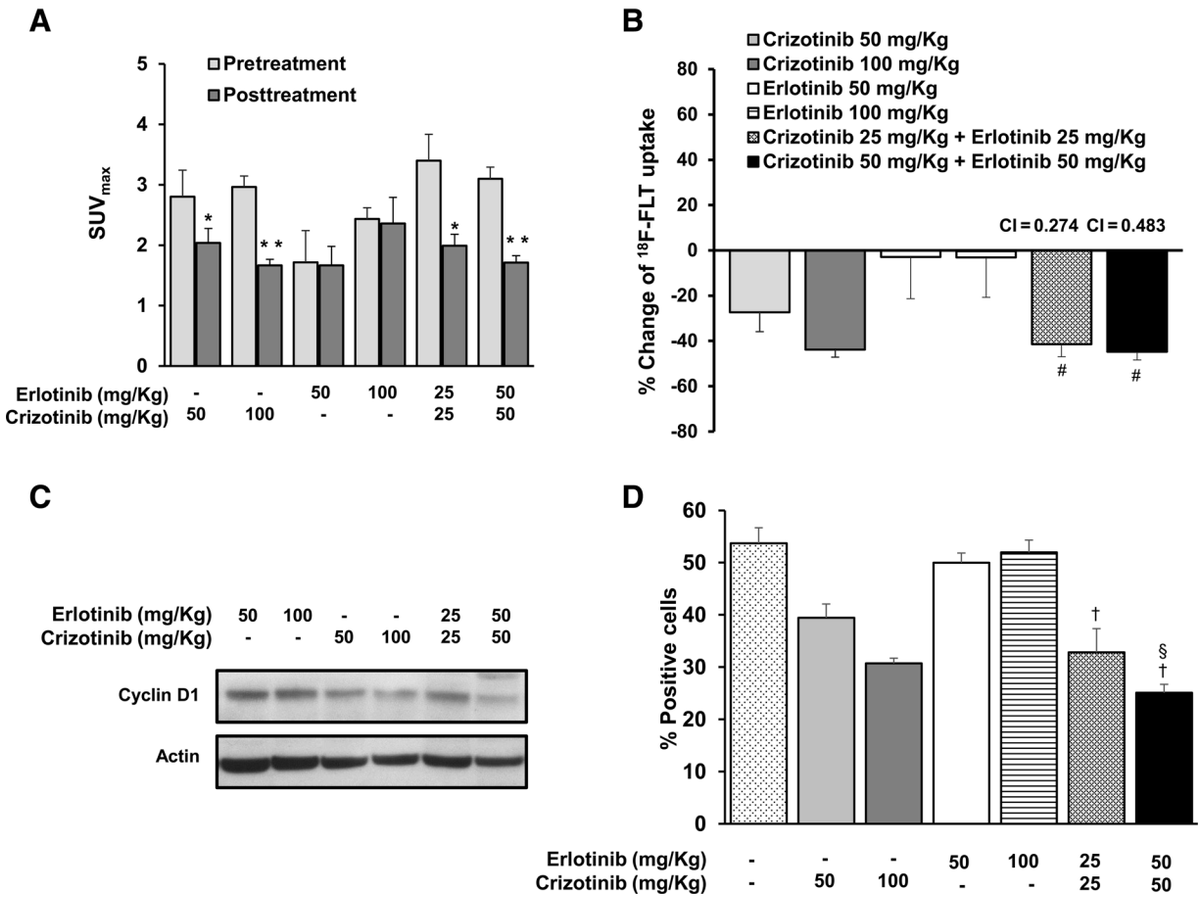

Figure 4.

Quantitative analysis of ^{18}F-FLT uptake in xenografts and proliferation markers in excised tumors. **A,** SUV_{max} values of pre- and posttreatment scans in H1993 tumor-bearing animals are reported and statistically compared (*, $P < 0.05$; **, $P < 0.01$ treated vs. untreated). **B,** percentage variations of ^{18}F-FLT uptake in H1993 tumor-bearing animals in response to treatment with single agent or with escalating dose of combined treatment. #, $P < 0.05$ combined treatment vs. 50 mg/kg crizotinib. **C,** levels of cyclin D1 in whole lysates of H1993 tumors. Actin levels were shown to ensure equal loading. **D,** percentage of positive cells at Ki67 staining of tumor sections (§, $P < 0.05$ combined treatment vs .100 mg/kg crizotinib; †, $P < 0.05$ combined treatment vs. 50 mg/kg crizotinib).

whereas no changes of IP3R3 levels were observed in response to erlotinib alone. Fig. 5D shows the time-dependent modulation of IP3R3 in H1993 cells exposed to 1 μmol/L crizotinib or erlotinib. Levels of IP3R3 were almost unchanged after 24 hours treatment with both agents whereas a time-dependent downregulation of IP3R3 was observed after treatment with crizotinib for 48 and 72 hours.

To test a cause–effect relationship between reduction of IP3R3 and enhanced efficacy of EGFR and MET inhibitors, we downregulated the expression of IP3R3 using scrambled and IP3R3-targeted siRNA in H1993 cells that were subsequently exposed to treatment with erlotinib (1 μmol/L) or crizotinib (1 μmol/L) for 24 hours. Fig. 6A shows the levels of IP3R3, total and phosphorylated forms of AKT and ERK1/2, p-STAT3^{Tyr705} as well as c-Myc and cyclin D1. As expected targeted siRNA caused a significant reduction of IP3R3 levels whereas no changes were observed in cells transfected with scrambled siRNA. Downregulation of IP3R3 in untreated cells do not cause any detectable change in the levels of signaling mediators and effectors. The addition of crizotinib to targeted-siRNA transfected cells for 24 hours caused an enhanced reduction of all signaling mediators and effectors as compared to scrambled-siRNA transfected cells exposed to crizotinib. No detectable changes of the same proteins were observed after treatment with erlotinib in targeted-siRNA transfected cells as compared to the corresponding negative control. Results of densitometric analysis of Western blotting signal in three independent siRNA transfection experiments were reported in supplementary Table S1.

In parallel experiments, we examined levels of BIM, Bcl-xL, and cleaved PARP (Fig. 6B) and found an increase of BIM levels in samples silenced for IP3R3 and treated with crizotinib and erlotinib as compared to scrambled-siRNA transfected cells exposed to the same drugs, whereas cleaved PARP was detected only after treatment with crizotinib in IP3R3-targeted siRNA transfected cells.

Then we examined the effects of IP3R3 siRNA transfection followed by treatment with crizotinib and erlotinib on Ras, an upstream mediator in the signaling cascade triggered by EGFR and MET and in particular K-Ras, the isoform almost

Published OnlineFirst April 4, 2018; DOI: 10.1158/1078-0432.CCR-17-3657

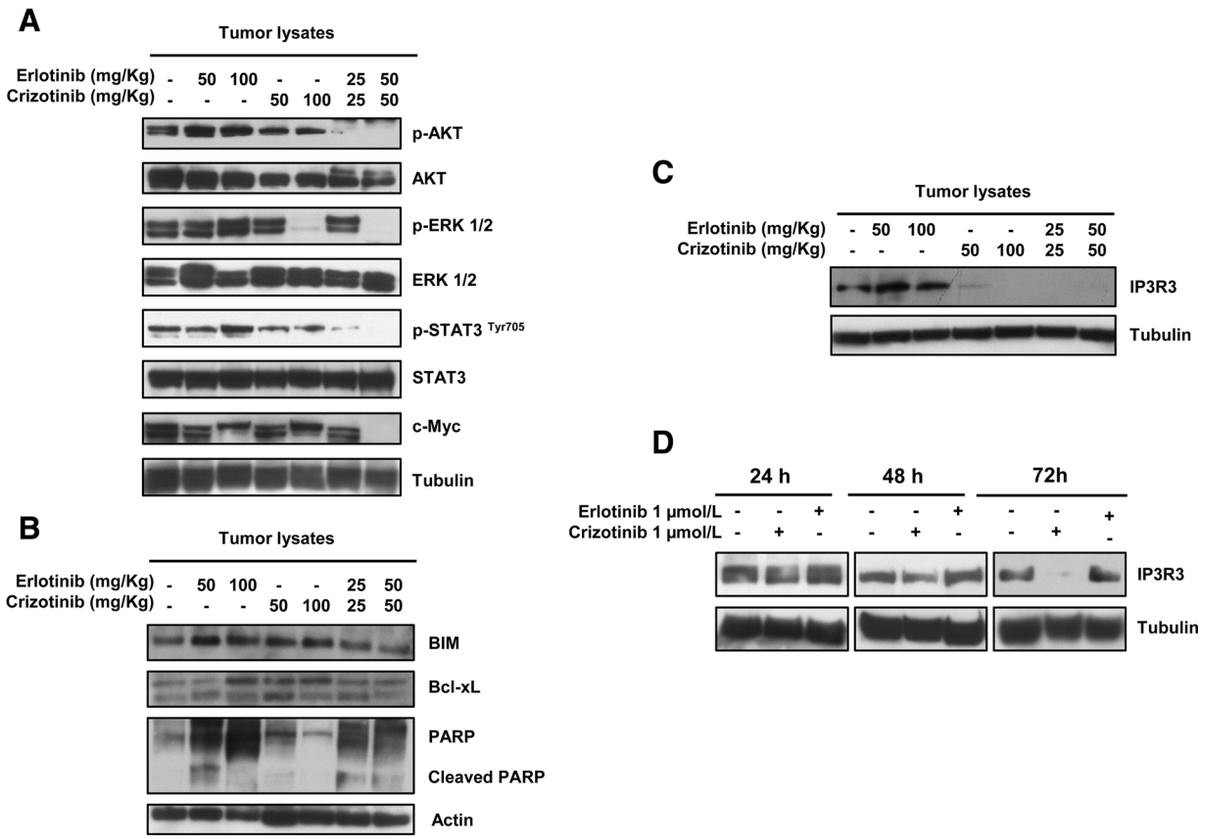

Figure 5.

Signaling cascade, apoptosis, and levels of IP3R3 in excised tumors. **A** and **B,** Western blot analysis of whole lysates from H1993 xenografts after 3 days treatment with erlotinib and crizotinib alone or in combination showing levels of signaling mediators (**A**) and markers of apoptosis (**B**). **C**, levels of IP3R3 in excised tumors after 3 days treatment with erlotinib or crizotinib alone or in combination. **D,** time-course of IP3R3 modulation by erlotinib and crizotinib in H1993 cells. A time-dependent decrease of IP3R3 levels were observed after 48 to 72 hours of treatment with crizotinib. Tubulin or actin were used to ensure equal loading.

exclusively expressed in H1993 cells (41). We found that 24 hours treatment with crizotinib combined with downregulation of IP3R3 caused a strong reduction of K-Ras levels in whole cell lysates (Fig. 6C). Notably, also erlotinib caused a considerable reduction of K-Ras levels after 24 hours treatment in combination with IP3R3 silencing. These observations may indicate that both drugs are able to modulate K-Ras when IP3R3 is downregulated. In particular, posttranscriptional regulation of Ras is reported to occur through its translocation from plasma membrane to different intracellular membrane microdomains including endoplasmic reticulum and Golgi apparatus (42). Then we tested whether crizotinib and erlotinib alone or in combination may affect activation of Ras. Fig. 6D shows that activated Ras is reduced by 24 hours treatment with crizotinib, erlotinib, or combination of both agents achieving the maximal effect with high dose combination therapy.

Because K-Ras, phosphorylated at serine 181, is reported to interact with inositol trisphosphate receptors, we immunoprecipitated IP3R3 from whole cell lysates of untreated and erlotinib treated (72 hours) H1993 cells and immunoprecipitated samples were simultaneously blotted for K-Ras and phospho-serine. We found that erlotinib treatment caused a reduction of direct or indirect interaction between IP3R3 and K-Ras mainly through the dephosphorylation of serine residues of K-Ras (Fig. 6E). These findings indicate that, despite resistance to erlotinib for *MET*-amplification, EGFR inhibitors may disrupt IP3R3 and K-Ras interaction thus reinforcing the effects of crizotinib.

Discussion

Our study showed that cotargeting of EGFR and MET receptors in resistant NSCLC caused enhanced inhibitory effects on signaling cascade and proliferation both in cells and tumors and these combined effects could be detected and quantitatively analyzed using ^{18}F-FLT PET/CT. Furthermore, our findings indicate that the enhanced efficacy of EGFR and MET inhibitors is mediated by IP3R3 and its interaction with K-Ras since crizotinib causes a strong downregulation of IP3R3 preventing binding of K-Ras to the endoplasmic reticulum and EGFR inhibitors decrease the interaction between IP3R3 and K-Ras mainly through the dephosphorylation of its serine residues.

The simultaneous targeting of EGFR and MET is a strategy currently adopted in clinical trials to prevent or overcome MET-mediated resistance to EGFR inhibitors in EGFR-driven NSCLC. However, two randomized studies with onartuzumab,

Published OnlineFirst April 4, 2018; DOI: 10.1158/1078-0432.CCR-17-3657

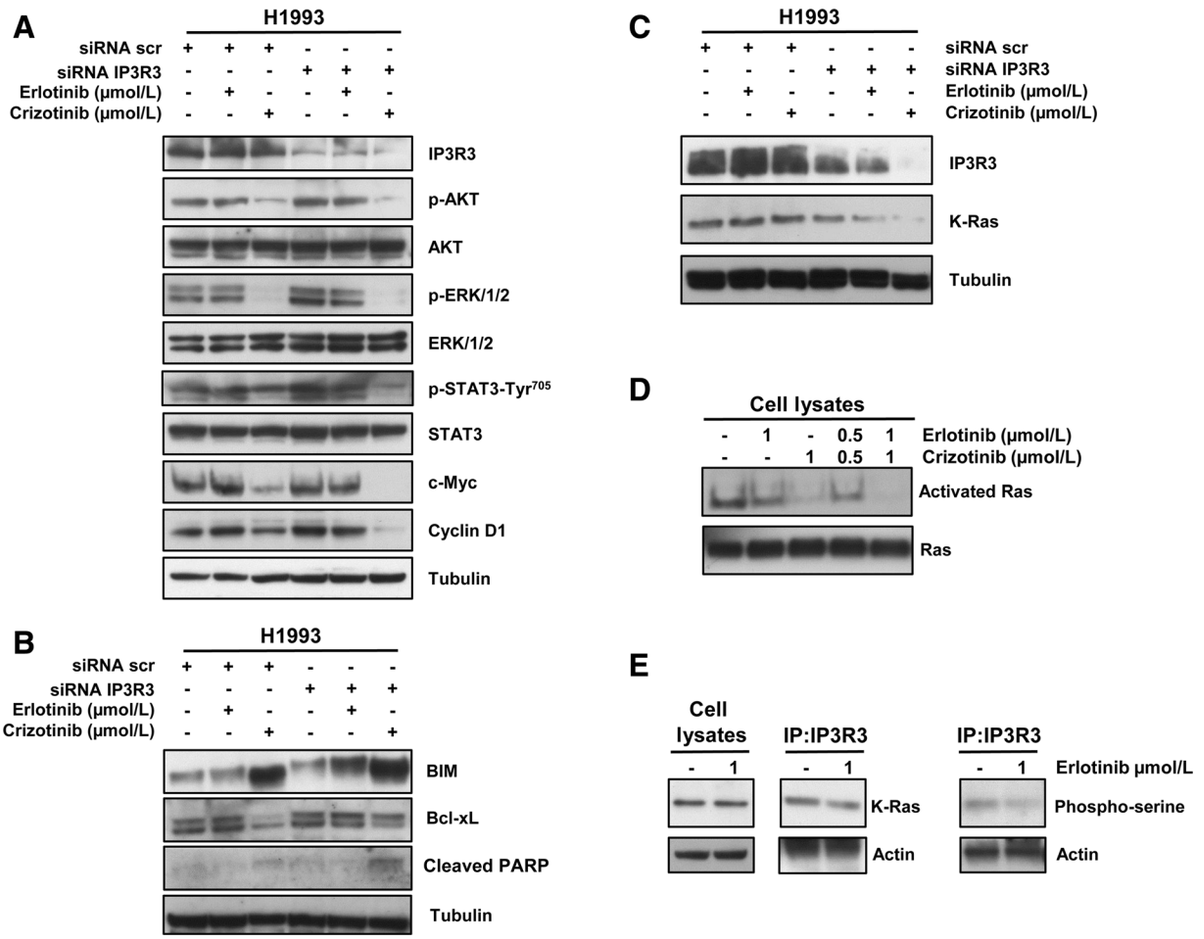

Figure 6.

Silencing of IP3R3 and response to EGFR and MET inhibitors in H1993 cells. Transfection of cells with IP3R3-targeted and scrambled siRNA was performed and after 48 hours they were treated with 1 μmol/L erlotinib, 1 μmol/L crizotinib or vehicle for additional 24 hours. **A,** levels of IP3R3, total and phosphorylated forms of AKT and ERK 1/2, $STAT3^{Tyr705}$ as well as c-Myc and cyclin D1 are shown. **B,** levels of BIM, Bcl-xL and cleaved PARP in the same samples. **C,** levels of K-Ras after silencing of IP3R3 and treatment with EGFR or MET inhibitors. **D,** levels of activated Ras in response to 24 hours treatment with erlotinib and crizotinib alone or in combination. **E**, interaction between IP3R3 and total K-Ras or serine phosphorylated forms of K-Ras. Whole lysates from untreated and 72 hours erlotinib treated cells were immunoprecipitated with anti-IP3R3 antibody and then simultaneously blotted for K-Ras and phospho-serine. Three independent experiments were performed. Tubulin or actin were used to ensure equal loading.

a monoclonal antibody competing with ligand for the binding to MET receptor, and tivatinib, a non-ATP competitive MET inhibitor, in combination with erlotinib did not show significant clinical activity in previously treated patients with advanced NSCLC (26, 43). It is important to note that patients were included in these studies without knowing their *MET* genetic status. In another randomized phase II study in which TKI-naïve patients were tested for molecular characteristics such as *MET* amplification, EGFR status, and K-Ras mutations, the combination of erlotinib and tivatinib was significantly effective in a subpopulation of patients having K-Ras mutations (25). On the basis of our observations, the cotargeting of EGFR and MET may provide maximal growth arrest in NSCLCs bearing *MET* amplification when the MET inhibitor is able to block the downstream signaling cascade and simultaneously downregulate IP3R3 whereas the co-administered EGFR TKI is able to cause serine dephosphorylation of K-Ras thus reducing its interaction with IP3R3.

Silencing of IP3R3 with targeted siRNA in combination with crizotinib or erlotinib caused a reduction of K-Ras levels. Previous studies reported indeed that IP3Rs interact with K-Ras4B, one of two splice variants of *K-Ras* gene (44). This interaction is reported to occur when K-Ras4B is GTP-bound and is enhanced by phosphorylation of K-Ras at serine 181 (44). When phosphorylated, K-Ras4B has a decreased net charge, a lower affinity for plasma membrane and can translocate to the endoplasmic reticulum where it may interact with IP3Rs (45). In our study, crizotinib treatment for 48 to 72 hours caused a dramatic reduction of IP3R3 levels, similar to that caused by targeted siRNA, thus preventing anchorage of K-Ras at the endoplasmic reticulum and favoring its redistribution in other membrane microdomains. Conversely, erlotinib treatment for 72 hours did not have any significant effect on IP3R3 levels but was able to reduce its interaction with K-Ras thus favoring again changes in K-Ras intracellular compartmentalization. Crizotinib- and erlotinib- induced relocation of K-Ras

Published OnlineFirst April 4, 2018; DOI: 10.1158/1078-0432.CCR-17-3657

in the same or different membrane microdomains may ultimately result in a reduced K-Ras activity.

Previous studies reported the interaction of IP3R3 with FBXL2, one of the components of ubiquitin ligase complexes, in response to H_2O_2 and serum restoration, leading to proteasome-mediated degradation of IP3R3 and limitation of Ca^{2+} influx into mitochondria (46, 47). Although we used different experimental conditions, we cannot exclude that downregulation of IP3R3 may be due to ubiquitin-mediated degradation. Because IP3R3-mediated Ca^{2+} transfer to mitochondria triggers apoptosis promoting the opening of mitochondrial permeability transition pore, the downregulation of IP3R3 in response to crizotinib may raise the concern that apoptosis could be impaired by the reduced levels of IP3R3. Although this issue was not the main purpose of this study, we could detect a slight increase of cleaved PARP levels in tumors treated for 3 days with combined regimens and in IP3R3-targeted siRNA transfected cells exposed to crizotinib for 24 hours. Furthermore, in an our previous study, we showed that gefitinib treatment caused an early and relative increase of cytosolic and mitochondrial Ca^{2+} levels through an IP3R3-mediated calcium release from the endoplasmic reticulum (33), suggesting that erlotinib may in part compensate the effects of crizotinib on intra-cellular Ca^{2+} dynamics.

In conclusion, our study provided consistent evidences of enhanced effects of EGFR and MET cotargeting in resistant NSCLC cells that could be detected in vivo by ^{18}F-FLT PET/CT. Furthermore, our findings highlighted the role of IP3R3 and its interaction with K-Ras as a multifunctional platform that is able to integrate simultaneous inhibitory signals of RTK pathways thus enhancing the effects of drug combination. A potential clinical implication of our observations could be to perform an imaging test to assess the efficacy of combination therapy by treating NSCLC patients for a short period of time with crizotinib alone and then add the EGFR inhibitor. The early enhancement of cotargeting efficacy could be revealed by ^{18}F-FLT PET/CT performed at baseline, after crizotinib and after combination therapy. Finally, our study provided clues for the rational combination of targeted agents and indicated that the role of IP3R3 and its interaction with K-Ras should be taken into account for the success of combined therapy in oncogene driven NSCLC.

Disclosure of Potential Conflicts of Interest

No potential conflicts of interest were disclosed.

Authors' Contributions

Conception and design: F. Iommelli, S. Del Vecchio
Development of methodology: F. Iommelli, V. De Rosa, C. Terlizzi, M. Panico
Acquisition of data (provided animals, acquired and managed patients, provided facilities, etc.): F. Iommelli, C. Terlizzi, M. Monti
Analysis and interpretation of data (e.g., statistical analysis, biostatistics, computational analysis): F. Iommelli, V. De Rosa, R. Fonti, S. Del Vecchio
Writing, review, and/or revision of the manuscript: F. Iommelli, R. Fonti, S. Del Vecchio
Study supervision: S. Del Vecchio

Acknowledgments

This work was partly supported by Associazione Italiana per la Ricerca sul Cancro (AIRC, project No. IG-17249) and Programma Operativo Regionale POR Campania, Fondo Europeo Sviluppo Regionale 2007/2013, Rete delle Biotecnologie Campane.

The costs of publication of this article were defrayed in part by the payment of page charges. This article must therefore be hereby marked *advertisement* in accordance with 18 U.S.C. Section 1734 solely to indicate this fact.

Received December 6, 2017; revised March 6, 2018; accepted March 23, 2018; published first April 4, 2018.

References

1. Weinstein IB, Joe A. Oncogene addiction. Cancer Res 2008;68:3077–80; discussion 80.
2. Sharma SV, Settleman J. Oncogene addiction: setting the stage for molecularly targeted cancer therapy. Genes Dev 2007;21:3214–31.
3. Pao W, Girard N. New driver mutations in non-small-cell lung cancer. Lancet Oncol 2011;12:175–80.
4. Sequist LV, Waltman BA, Dias-Santagata D, Digumarthy S, Turke AB, Fidias P, et al. Genotypic and histological evolution of lung cancers acquiring resistance to EGFR inhibitors. Sci Transl Med 2011;3:75ra26.
5. Crystal AS, Shaw AT, Sequist LV, Friboulet L, Niederst MJ, Lockerman EL, et al. Patient-derived models of acquired resistance can identify effective drug combinations for cancer. Science 2014;346:1480–6.
6. Yap TA, Omlin A, de Bono JS. Development of therapeutic combinations targeting major cancer signaling pathways. J Clin Oncol 2013;31:1592–605.
7. Al-Lazikani B, Banerji U, Workman P. Combinatorial drug therapy for cancer in the post-genomic era. Nat Biotechnol 2012;30:679–92.
8. Pao W, Chmielecki J. Rational, biologically based treatment of EGFR-mutant non-small-cell lung cancer. Nat Rev Cancer 2010;10:760–74.
9. Lee SM, Khan I, Upadhyay S, Lewanski C, Falk S, Skailes G, et al. First-line erlotinib in patients with advanced non-small-cell lung cancer unsuitable for chemotherapy (TOPICAL): a double-blind, placebo-controlled, phase 3 trial. Lancet Oncol 2012;13:1161–70.
10. Peters S, Adjei AA, Gridelli C, Reck M, Kerr K, Felip E, et al. Metastatic non-small-cell lung cancer (NSCLC): ESMO clinical practice guidelines for diagnosis, treatment and follow-up. Ann Oncol 2012;23:vii56–64.
11. Zhou C, Wu YL, Chen G, Feng J, Liu XQ, Wang C, et al. Erlotinib versus chemotherapy as first-line treatment for patients with advanced EGFR mutation-positive non-small-cell lung cancer (OPTIMAL, CTONG-0802): a multicentre, open-label, randomised, phase 3 study. Lancet Oncol 2011;12:735–42.
12. Ohashi K, Maruvka YE, Michor F, Pao W. Epidermal growth factor receptor tyrosine kinase inhibitor-resistant disease. J Clin Oncol 2013;31:1070–80.
13. Engelman JA, Zejnullahu K, Mitsudomi T, Song Y, Hyland C, Park JO, et al. MET amplification leads to gefitinib resistance in lung cancer by activating ERBB3 signaling. Science 2007;316:1039–43.
14. Engelman JA, Janne PA. Mechanisms of acquired resistance to epidermal growth factor receptor tyrosine kinase inhibitors in non-small cell lung cancer. Clin Cancer Res 2008;14:2895–9.
15. Chabon JJ, Simmons AD, Lovejoy AF, Esfahani MS, Newman AM, Haringsma HJ, et al. Circulating tumour DNA profiling reveals heterogeneity of EGFR inhibitor resistance mechanisms in lung cancer patients. Nat Commun 2016;7:11815.
16. Xu L, Kikuchi E, Xu C, Ebi H, Ercan D, Cheng KA, et al. Combined EGFR/MET or EGFR/HSP90 inhibition is effective in the treatment of lung cancers codriven by mutant EGFR containing T790M and MET. Cancer Res 2012;72:3302–11.
17. Suda K, Murakami I, Katayama T, Tomizawa K, Osada H, Sekido Y, et al. Reciprocal and complementary role of MET amplification and EGFR T790M mutation in acquired resistance to kinase inhibitors in lung cancer. Clin Cancer Res 2010;16:5489–98.

Published OnlineFirst April 4, 2018; DOI: 10.1158/1078-0432.CCR-17-3657

18. Bean J, Brennan C, Shih JY, Riely G, Viale A, Wang L, et al. MET amplification occurs with or without T790M mutations in EGFR mutant lung tumors with acquired resistance to gefitinib or erlotinib. Proc Natl Acad Sci U S A 2007;104:20932–7.
19. Sadiq AA, Salgia R. MET as a possible target for non-small-cell lung cancer. J Clin Oncol 2013;31:1089–96.
20. Gherardi E, Birchmeier W, Birchmeier C, Vande Woude G. Targeting MET in cancer: rationale and progress. Nat Rev Cancer 2012;12:89–103.
21. Blumenschein GR Jr., Mills GB, Gonzalez-Angulo AM. Targeting the hepatocyte growth factor-cMET axis in cancer therapy. J Clin Oncol 2012;30:3287–96.
22. Schildhaus HU, Schultheis AM, Ruschoff J, Binot E, Merkelbach-Bruse S, Fassunke J, et al. MET amplification status in therapy-naive adeno- and squamous cell carcinomas of the lung. Clin Cancer Res 2015;21:907–15.
23. Salgia R. MET in lung cancer: biomarker selection based on scientific rationale. Mol Cancer Ther 2017;16:555–65.
24. Turke AB, Zejnullahu K, Wu YL, Song Y, Dias-Santagata D, Lifshits E, et al. Preexistence and clonal selection of MET amplification in EGFR mutant NSCLC. Cancer Cell 2010;17:77–88.
25. Sequist LV, von Pawel J, Garmey EG, Akerley WL, Brugger W, Ferrari D, et al. Randomized phase II study of erlotinib plus tivantinib versus erlotinib plus placebo in previously treated non-small-cell lung cancer. J Clin Oncol 2011;29:3307–15.
26. Scagliotti G, von Pawel J, Novello S, Ramlau R, Favaretto A, Barlesi F, et al. Phase III multinational, randomized, double-blind, placebo-controlled study of tivantinib (ARQ 197) plus erlotinib versus erlotinib alone in previously treated patients with locally advanced or metastatic nonsquamous non-small-cell lung cancer. J Clin Oncol 2015;33:2667–74.
27. Gainor JF, Niederst MJ, Lennerz JK, Dagogo-Jack I, Stevens S, Shaw AT, et al. Dramatic response to combination erlotinib and crizotinib in a patient with advanced, EGFR-mutant lung cancer harboring De Novo MET amplification. J Thorac Oncol 2016;11:e83–5.
28. Iommelli F, De Rosa V, Gargiulo S, Panico M, Monti M, Greco A, et al. Monitoring reversal of MET-mediated resistance to EGFR tyrosine kinase inhibitors in non-small cell lung cancer using 3′-deoxy-3′-[18F]-fluorothymidine positron emission tomography. Clin Cancer Res 2014;20:4806–15.
29. Zannetti A, Iommelli F, Speranza A, Salvatore M, Del Vecchio S. 3′-deoxy-3′-18F-fluorothymidine PET/CT to guide therapy with epidermal growth factor receptor antagonists and Bcl-xL inhibitors in non-small cell lung cancer. J Nucl Med 2012;53:443–50.
30. Iommelli F, De Rosa V, Fonti R, Del Vecchio S. Molecular imaging for detection of sensitivity and resistance to EGFR tyrosine kinase inhibitors in non-small cell lung cancer. Clin Transl Imaging 2014;2:43–53.
31. Kubo T, Yamamoto H, Lockwood WW, Valencia I, Soh J, Peyton M, et al. MET gene amplification or EGFR mutation activate MET in lung cancers untreated with EGFR tyrosine kinase inhibitors. Int J Cancer 2009;124:1778–84.
32. De Rosa V, Iommelli F, Monti M, Fonti R, Votta G, Stoppelli MP, et al. Reversal of warburg effect and reactivation of oxidative phosphorylation by differential inhibition of EGFR signaling pathways in non-small cell lung cancer. Clin Cancer Res 2015;21:5110–20.
33. Zannetti A, Iommelli F, Fonti R, Papaccioli A, Sommella J, Lettieri A, et al. Gefitinib induction of in vivo detectable signals by Bcl-2/Bcl-xL modulation of inositol trisphosphate receptor type 3. Clin Cancer Res 2008;14:5209–19.
34. Oh SJ, Mosdzianowski C, Chi DY, Kim JY, Kang SH, Ryu JS, et al. Fully automated synthesis system of 3′-deoxy-3′-[18F]fluorothymidine. Nucl Med Biol 2004;31:803–9.
35. Fonti R, Larobina M, Del Vecchio S, De Luca S, Fabbricini R, Catalano L, et al. Metabolic tumor volume assessed by 18F-FDG PET/CT for the prediction of outcome in patients with multiple myeloma. J Nucl Med 2012;53:1829–35.
36. De Rosa V, Iommelli F, Monti M, Mainolfi CG, Fonti R, Del Vecchio S. Early (18)F-FDG uptake as a reliable imaging biomarker of T790M-mediated resistance but not MET amplification in non-small cell lung cancer treated with EGFR tyrosine kinase inhibitors. EJNMMI Res 2016;6:74.
37. Chou TC. Drug combination studies and their synergy quantification using the Chou-Talalay method. Cancer Res 2010;70:440–6.
38. Chou TC. Theoretical basis, experimental design, and computerized simulation of synergism and antagonism in drug combination studies. Pharmacol Rev 2006;58:621–81.
39. Lemmon MA, Schlessinger J. Cell signaling by receptor tyrosine kinases. Cell 2010;141:1117–34.
40. Akl H, Bultynck G. Altered Ca(2+) signaling in cancer cells: proto-oncogenes and tumor suppressors targeting IP3 receptors. Biochim Biophys Acta 2013;1835:180–93.
41. Lutterbach B, Zeng Q, Davis LJ, Hatch H, Hang G, Kohl NE, et al. Lung cancer cell lines harboring MET gene amplification are dependent on Met for growth and survival. Cancer Res 2007;67:2081–8.
42. Omerovic J, Prior IA. Compartmentalized signalling: Ras proteins and signalling nanoclusters. FEBS J 2009;276:1817–25.
43. Spigel DR, Edelman MJ, O'Byrne K, Paz-Ares L, Mocci S, Phan S, et al. Results from the phase III randomized trial of onartuzumab plus erlotinib versus erlotinib in previously treated stage IIIB or IV non-small-cell lung cancer: METLung. J Clin Oncol 2017;35:412–20.
44. Sung PJ, Tsai FD, Vais H, Court H, Yang J, Fehrenbacher N, et al. Phosphorylated K-Ras limits cell survival by blocking Bcl-xL sensitization of inositol trisphosphate receptors. Proc Natl Acad Sci U S A 2013;110:20593–8.
45. Ahearn IM, Haigis K, Bar-Sagi D, Philips MR. Regulating the regulator: post-translational modification of RAS. Nat Rev Mol Cell Biol 2011;13:39–51.
46. Kuchay S, Giorgi C, Simoneschi D, Pagan J, Missiroli S, Saraf A, et al. PTEN counteracts FBXL2 to promote IP3R3- and Ca(2+)-mediated apoptosis limiting tumour growth. Nature 2017;546:554–58.
47. Bononi A, Giorgi C, Patergnani S, Larson D, Verbruggen K, Tanji M, et al. BAP1 regulates IP3R3-mediated Ca(2+) flux to mitochondria suppressing cell transformation. Nature 2017;546:549–53.

Published OnlineFirst April 4, 2018; DOI: 10.1158/1078-0432.CCR-17-3657

Clinical Cancer Research

Inositol Trisphosphate Receptor Type 3-mediated Enhancement of EGFR and MET Cotargeting Efficacy in Non–Small Cell Lung Cancer Detected by ^{18}F-fluorothymidine

Francesca Iommelli, Viviana De Rosa, Cristina Terlizzi, et al.

Clin Cancer Res 2018;24:3126-3136. Published OnlineFirst April 4, 2018.